Journal of Energy

VOLUME 72 Number 4 | 2023

journal homepage: http://journalofenergy.com/

3D Acoustic Heat-Maps for Transformer Monitoring Applications

Ferdinand Fuhrmann, Anna Maly, Martin Blass, Jakub Waikat, Fredi Belavić, Franz Graf

***Summary* — We present a novel approach for measuring and representing acoustic emissions of transformers. The representation of location-based acoustic emissions enables improved monitoring of transformers, e.g., to detect and predict anomalies and failure events. Here, we introduce 3D acoustic heatmaps to visualize the sound emission patterns of a transformer. We use a combined sensing approach consisting of a 3D point cloud, a microphone array, and beamforming algorithms to generate the distributed representation of acoustic emissions over the entire surface of the transformer. In a further step, we intend to apply machine learning methods to the generated data to enable early fault prevention and predictive maintenance.**

***Keywords* — Transformer, Audio, Microphone Array, Monitoring.**

I. Introduction

Transformers are important building blocks of the electrical transmission system. Failure of these components can result in long outages as well as high restoration costs for the grid operator. Therefore, monitoring the condition of transformers and predicting potential failure events are of great interest to all involved parties. A successful monitoring system can thus minimize downtime and prevent transformer failure by triggering tailored predictive maintenance. The most common transformer monitoring techniques include thermal analysis, winding vibration, motion and deformation analysis, dissolve gas analysis, partial discharge analysis, and tapping under load analysis [1].

II. Background

Transformers emit characteristic noise due to the electromagnetic oscillatory behavior of various internal components [2]. These include core and coil oscillations. In addition, partial discharges in the winding insulation and insulating brushes contribute to the noise emissions [3]. Moreover, geomagnetically induced currents and other DC components of the core cause additional noise sources [4]. The combination of the aforementioned factors creates a complex sound field that is further influenced by the age of the transformer, its loading, and potential anomalies [5]. In this paper, a novel approach is developed to use the sound emission patterns of a transformer to represent and monitor the transformer condition during operation. Modelling the acoustic emissions of a transformer enables the detection and prediction of anomalies and failure events. With the here- presented system concept, we introduce additional information for transformer monitoring systems that established methods do not take into account (see Section 1).

III. System Overview

We present a novel approach to measure and visualize transformer acoustic emissions. We use the term 3D acoustic heatmap because we visualize the distribution of acoustic emissions over the entire surface of a transformer.

A lidar-generated 3D model of the transformer consists of uniformly distributed voxels. A beamformer algorithm calculates the directional sound radiation of each voxel. The values of the directional sound radiation result in a 3D acoustic heatmap for each desired frequency. These acoustic heatmaps show various information about different parameters, including the distributed sound pressure levels as well as the local sound sources at characteristic frequencies. Using this information, we can create powerful visualization, inspection, and prediction models to assess the condition of the transformer.

IV. Wave Propagation Considerations

Spherical Wave versus Planar Wave. The use of a depth camera provides a great opportunity to use the information about the exact distance of the observed transformer voxels as possible sound sources to each microphone. Usually, it is assumed that the aperture size of a microphone array is small compared to the distance to the sound source. In our case, however, it is not. The Direction of Arrival (DOA) error of the assumed plane wave is therefore no longer negligible.

Figure 1 shows the error of the assumed plane wave. The sound travels from sound source to two microphones, separated by distance d, via r_1 and r_2. We choose the first microphone as the reference microphone, so the plane wave is orthogonal to r_1 and φ is the arrival angle. It can be easily seen that $DOA_{Sphere} = r_2 - r_1$, while $DOA_{Planar} = d \cos \varphi$. Considering the cosine rule, the error resulting from the plane wave assumption depends on three parameters, φ, r_1 and d, respectively.

(Corresponding author: Ferdinand Fuhrmann)

Ferdinand Fuhrmann, Anna Maly, Martin Blass and Franz Graf are with the JOANNEUM RESEARCH Forschungsgesellschaft mbH, Graz, Austria (e-mails: ferdinand.fuhrmann@joanneum.at, anna.maly@joanneum.at, martin.blass@joanneum.at, franz.graf@joanneum.at)

Jakub Waikat is with the Siemens Energy GmbH, Vienna, Austria (e-mail: jakub.waikat@siemens-energy.com)

Fredi Belavic is with the Austrian Power Grid AG, Vienna, Austria (e-mail: fredi.belavic@apg.at)

Ferdinand Fuhrmann, Anna Maly, Martin Blass, Jakub Waikat, Fredi Belavić, Franz Graf, 3D Acoustic Heat-Maps for Transformer Monitoring Applications, Journal of Energy, vol. 72 Number 4 (2023), 15–18
https://doi.org/10.37798/2023724508

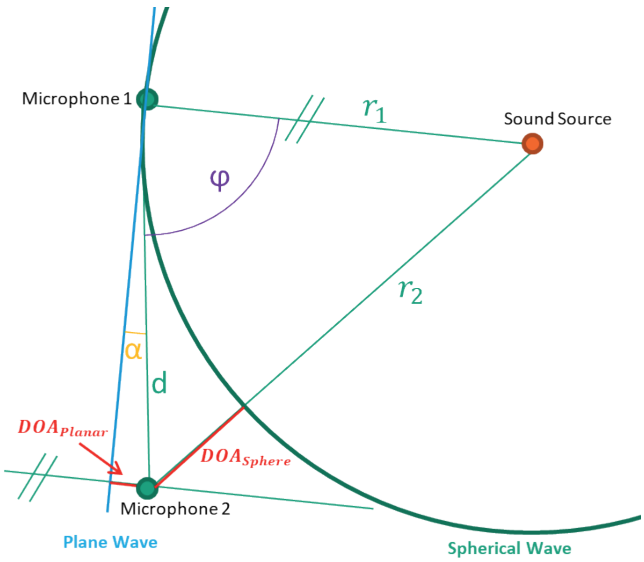

Fig. 1. Error of the plane wave assumption

Figure 2 shows the DOA error at different sound source distances and different microphone distances while keeping the angle of arrival at 80°. Figure 3 shows the DOA error at various sound source distances and arrival angles while the microphone distance is kept at 1 m. The larger the sound source distance, the smaller the error. Moreover, the influence of the error is frequency-dependent; for frequencies with large wavelengths compared to the DOA error, the effect of assuming a plane wave is smaller than for frequencies with small wavelengths, i.e., high frequencies are more affected than low frequencies. A microphone array with an aperture size of about 1 m, a common r1 of 5 m, and an angle of arrival of about 70° has a plane-wave assumption error of around 0.1 m. At 500 Hz, this becomes a wavelength error of about 52°, with 180° representing complete negative interference. The use of a point cloud as possible sound source points gives excellent results for acoustic heat maps and avoids these errors in assuming plane waves.

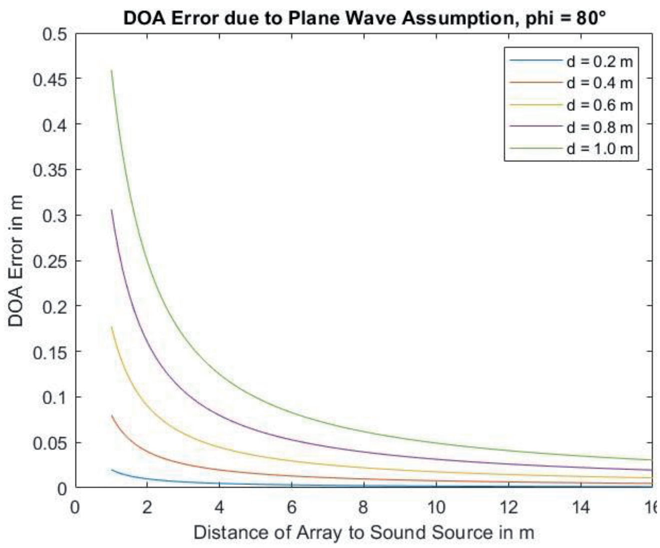

Fig. 2. Error at arrival angle 80°

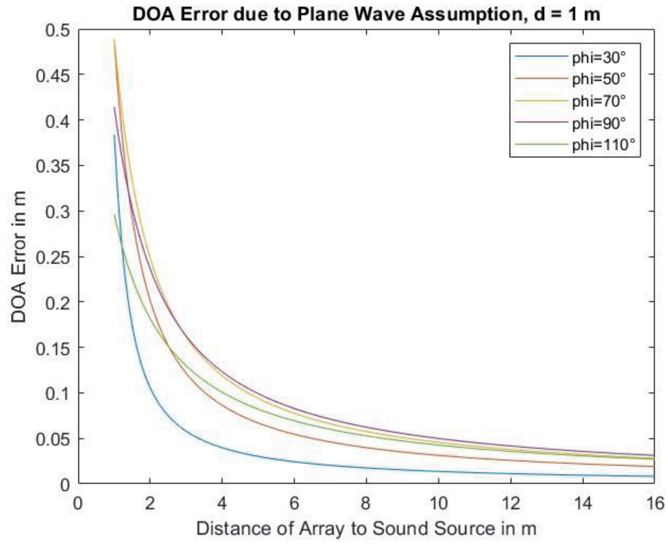

Fig. 3. Error at a microphone interdistance of 1m

V. Implementation

The proposed information processing system consists of a 3D model of the transformer created using a LIDAR scan, a microphone array for audio acquisition, and a beamforming algorithm for processing the multichannel audio data. In the following, we describe the above-mentioned components in detail.

3D Modelling. A 3D model of the transformer created from a LIDAR omnidirectional scan serves as a starting point. Using an RGB-D image taken with a combined visual sensor (RGB and depth), we then register the actual position of the microphone array with respect to the 3D model. In this way, we ensure optimal matching of the different sensor modalities, resulting in the best possible mapping of the audio data to the point cloud.

Microphone Array. The microphone array has a special 3D design that takes into account the desired characteristics in terms of sound distribution as well as mechanical stability and durability.

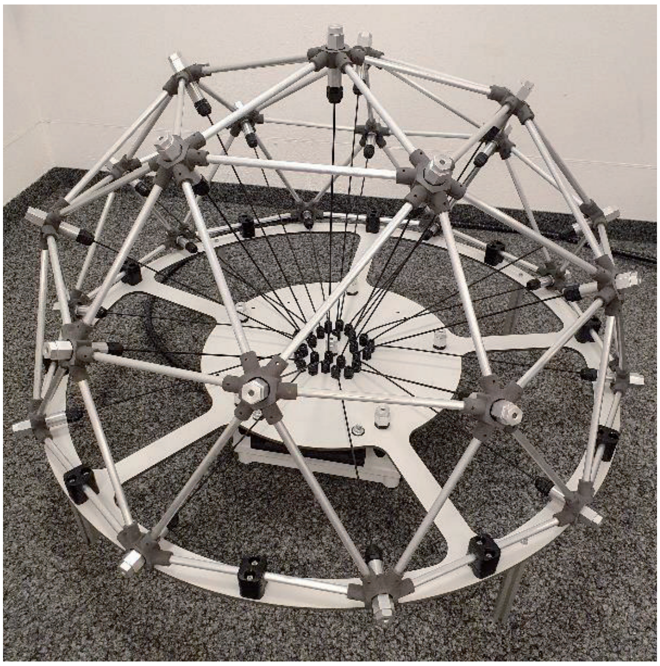

Fig. 4. 32-channel microphone array construction in icosahedron dome geometry.

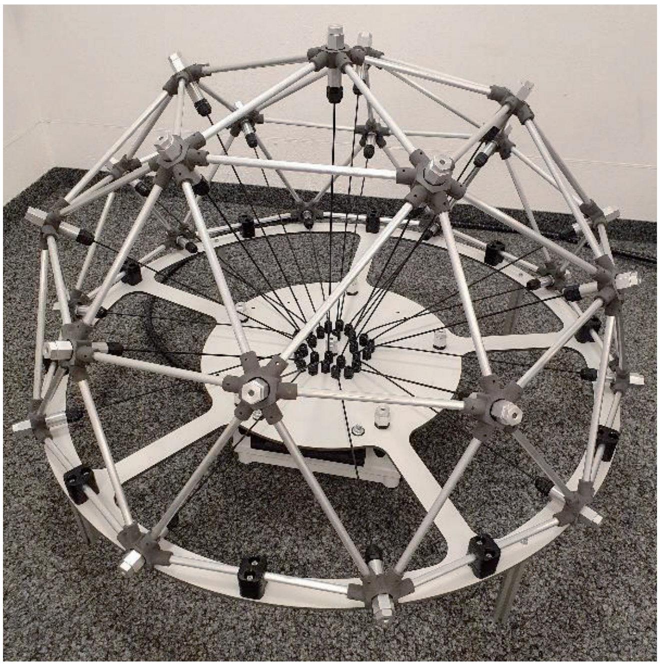

Fig.5. ICP electret microphone inside IP67 enclosure

The geometry consists of an icosahedron dome V2 [6][7] with a radius of 135 cm and 26 vertices mounted on a base plate with 6 holes. This results in 32 sensor positions for ICP electret microphones in an IP67 enclosure. The array geometry was chosen based on numerical beamforming simulations to achieve an appropriate tradeoff between main lobe width and maximum sidelobe levels for third-octave center frequencies within 100 Hz and 20 kHz, resulting in a directivity index greater than 10 dB for frequencies above 200 Hz and greater than 15 dB for frequencies above 800 Hz. The effective spatial aliasing-free frequency range with minimal directionality is 130 Hz to 15 kHz [8]. Fig. 4 and 5 show the array design and the microphone enclosures used for data acquisition.

Beamforming. We use delay-and-sum (DAS) beamforming [9] to compute the sound arriving from a given direction. Beside its straightforward implementation, DAS guarantees artifact-free output signals, which is important for any acoustic modelling approach that relies on these signals. Furthermore, DAS preserves the amplitude ratios with respect to the input signals, which is mandatory for the calculation of the resulting absolute sound pressure values. The use of the 3D point cloud outperforms the typically assumed plane wave, especially for short distances between the microphone array and the transformer. The voxels on the transformer surface serve as sound source positions for the beamforming algorithm. Therefore, the correct spacing of the 3D point cloud significantly improves the radiation pattern.

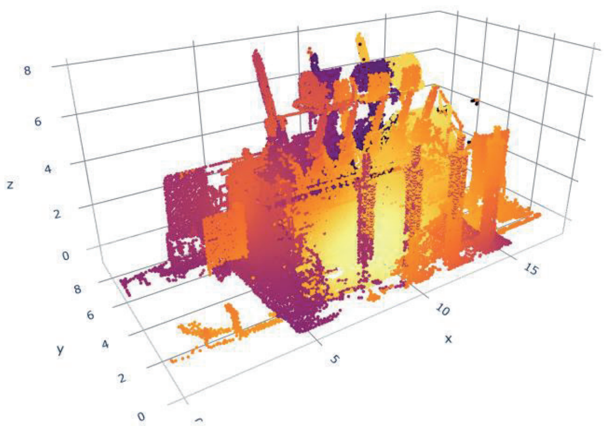

Fig. 6. 3D Heatmap representing the transfomer sound emmissions.

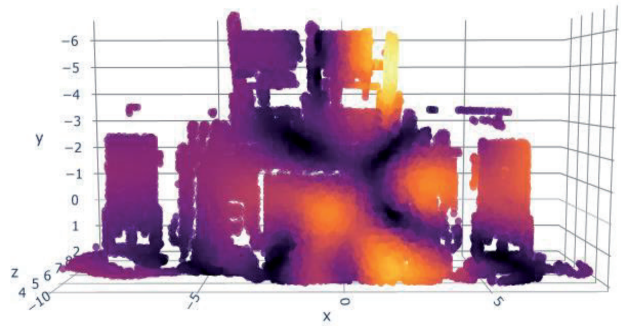

Fig. 7. Broadside heatmap of the transformer for 600Hz.

Fig. 8: Microphone array mounted on a mobile robot during measurements in a substation.

The obtained sound radiation pattern represents the sound radiation of the transformer at the microphone array position. Although we assume the main sound radiation in the orthogonal directions of the transformer, the study of the anisotropic behavior will be a future step. Fig. 6 and 7 show acoustic heatmaps of a transformer for the entire frequency range and a single frequency, respectively. Fig. 8 shows the used microphone array mounted on a mobile robot for data acquisition in a substation.

VI. Results

As a first result, we use the generated 3D acoustic heatmaps to investigate the sound radiation patterns over several characteristic frequencies. In practical applications, we use the system to scan each side of the transformer; the resulting heat maps visualize the all-around radiation patterns at each frequency.

Ferdinand Fuhrmann, Anna Maly, Martin Blass, Jakub Waikat, Fredi Belavić, Franz Graf, 3D Acoustic Heat-Maps for Transformer Monitoring Applications, Journal of Energy, vol. 72 Number 4 (2023), 15–18
https://doi.org/10.37798/2023724508

VII. Conclusions And Outlook

We have presented a novel approach for monitoring the condition of a transformer by creating 3D acoustic heat maps from acoustic sensor data. By combining data from a microphone array with a 3D model of the transformer, we have developed a powerful tool for inspection and modelling. In a next step, we aim to build predictive models by applying machine learning techniques to 3D acoustic heat maps collected during an automated measurement campaign over 3 months [10]. With these models, we aim to automatically predict anomalies as well as potential failure events by analyzing the acoustic radiation patterns emitted by the transformer.

Aknowledgements

This research is funded by the Austrian Research Promotion Agency (FFG) within the project XAMINOR

(881186) and the FFG-COMET-K1 Center "Pro2Future" (Products and Production Systems of the Future), Contract No. 881844.

References

[1] Moravej, Z., and S. Bagheri. "Condition monitoring techniques of power transformers: A review." *Journal of operation and Automation in power Engineering* 3.1 (2015): 71-82.J. Clerk Maxwell, *A Treatise on Electricity and Magnetism,* 3rd ed., vol. 2. Oxford: Clarendon, 1892, pp. 68-73.

[2] Jingzhu, Hu, et al. "Electromagnetic vibration noise analysis of transformer windings and core." *IET Electric Power Applications*10.4 (2016): 251-257.

[3] Bartoletti, Cipriano, et al. "Vibro-acoustic techniques to diagnose power transformers." *IEEE Transactions on Power Delivery* 19.1 (2004): 221- 229.

[4] Bailey, Rachel L., et al. "Modelling geomagnetically induced currents in midlatitude Central Europe using a thin-sheet approach." *Annales Geophysicae*. Vol. 35. No. 3. Göttingen, Germany: Copernicus Publications, 2017.

[5] Tenbohlen, Stefan, et al. "Diagnostic measurements for power transformers." *Energies* 9.5 (2016): 347.

[6] https://en.wikipedia.org/wiki/Icosahedron

[7] https://simplydifferently.org/Geodesic_Dome_Notes?page=3#2V/L2%20 Icosahedron%20Dome

[8] Brandstein M., and Ward D. "Microphone Arrays: signal processing techniques and applications." *Springer Science & Business Media* (2001)

[9] Elko, Gary W., and Jens Meyer. "Microphone arrays." *Springer handbook of speech processing* (2008): 1021-1041.

[10] Waikat, J., Jelidi, A., Lic, S., Sopidis, G., Kähler, O., Maly, A., Pestana, J., Fuhrmann, F., Belavic, F. "Preliminary Results by a Multi-Sensor Robot for the Lifecycle Monitoring of Transformers" In Proceedings of the 6th International Colloquium on Transformer Research and Asset Management (ICTRAM), 2023.

https://doi.org/10.37798/2023724508